Searching for globular cluster chemical anomalies on the main sequence of a young massive cluster

I. Cabrera-Ziri [iD],[1][*][†] J. S. Speagle [iD],[1] E. Dalessandro,[2] C. Usher [iD],[3,4] N. Bastian,[3]
M. Salaris,[3] S. Martocchia,[3,5] V. Kozhurina-Platais,[6] F. Niederhofer,[7] C. Lardo [iD],[8]
S. S. Larsen[9] and S. Saracino [iD][3]

[1]*Center for Astrophysics | Harvard & Smithsonian, 60 Garden Street, Cambridge, MA 02138, USA*
[2]*INAF-Osservatorio di Astrofisica e Scienza dello Spazio di Bologna, Via Gobetti 93/3, I-40129 Bologna, Italy*
[3]*Astrophysics Research Institute, Liverpool John Moores University, 146 Brownlow Hill, Liverpool L3 5RF, UK*
[4]*Department of Astronomy, Oskar Klein Centre, Stockholm University, AlbaNova University Centre, SE-106 91 Stockholm, Sweden*
[5]*European Southern Observatory, Karl-Schwarzschild-Strasse 2, D-85748 Garching bei München, Germany*
[6]*Space Telescope Science Institute, 3700 San Martin Drive, Baltimore, MD 21218, USA*
[7]*Leibniz-Institut für Astrophysik Potsdam (AIP), An der Sternwarte 16, D-14482 Potsdam, Germany*
[8]*Laboratoire d'Astrophysique, Ecole Polytechnique Fédérale de Lausanne, Observatoire de Sauverny, CH-1290 Versoix, Switzerland*
[9]*Department of Astrophysics/IMAPP, Radboud University, PO Box 9010, NL-6500 GL Nijmegen, the Netherlands*

ABSTRACT

The spectroscopic and photometric signals of the star-to-star abundance variations found in globular clusters seem to be correlated with global parameters like the cluster's metallicity, mass, and age. Understanding this behaviour could bring us closer to the origin of these intriguing abundance spreads. In this work we use deep *HST* photometry to look for evidence of abundance variations in the main sequence of a young massive cluster NGC 419 ($\sim10^5\,\mathrm{M_\odot}$, $\sim1.4\,\mathrm{Gyr}$). Unlike previous studies, *here we focus on stars in the same mass range found in old globulars* (~0.75–$1\,\mathrm{M_\odot}$), *where light elements variations are detected*. We find no evidence for N abundance variations among these stars in the $Un - B$ and $U - B$ colour–magnitude diagrams of NGC 419. This is at odds with the N variations found in old globulars like 47 Tuc, NGC 6352, and NGC 6637 with similar metallicity to NGC 419. Although the signature of the abundance variations characteristic of old globulars appears to be significantly smaller or absent in this young cluster, we cannot conclude if this effect is mainly driven by its age or its mass.

Key words: stars: abundances – Hertzsprung-Russell and colour–magnitude diagrams – globular clusters: general – globular clusters: individual: NGC 419, 47 Tuc, NGC 6352, NGC 6637 – galaxies: individual: SMC, Milky Way.

1 INTRODUCTION

The puzzle that is the origin of the star-to-star light element abundance variations within globular clusters (a.k.a. multiple stellar populations, MPs) is still unsolved. Since the beginning, an interesting piece of this puzzle has been the fact that clusters with similar metallicity can display very different ranges of their light element abundance variations (e.g. Kraft 1979). Large spectroscopic campaigns in the last decade have brought us a better understanding of the behaviour of some light elements as a function of global parameters, e.g. Carretta et al. (2010) found a correlation between the absolute magnitude of globular clusters (a proxy of their current mass) and the extent of some abundance distributions.

Similar findings have been produced by photometric studies using special filter combinations (a.k.a. pseudo-colours or supercolours) involving near-UV and/or blue (<4000 Å) filters which are able to pick up variations in the chemistry of the atmospheres (namely C, N, and O) and structure of the stars (consequence of different He mass fractions), e.g. Monelli et al. (2013). Arguably, Milone et al. (2017) with the use of *HST* supercolours provided the best picture to date of the manifestation of MPs in Galactic globulars as a function of global cluster properties like mass and metallicity. Understanding the physics of how such global parameters can regulate the expression of MPs at individual star level, e.g. how severe are the relative difference in the abundances of stars within a given cluster, could provide valuable insights into the origin of this phenomenon.

The role that age plays in the way MPs manifest has been difficult to constrain with Galactic targets. Studies of young open clusters have not found evidence for significant abundance variations among their stars (e.g. de Silva et al. 2009; Smiljanic et al. 2009; Pancino et al. 2010a; Carrera & Pancino 2011; Carrera & Martínez-Vázquez 2013; MacLean, De Silva & Lattanzio 2015). However, attributing this to an age effect is not straight forward for a couple of reasons: (1) there is a strong correlation between the cluster mass and the degree of change in light element abundance among cluster stars (e.g. Schiavon et al. 2013; Milone et al. 2017) and (2) metallicity is also known to modulate the signatures of MPs, with results suggesting that (on average) the abundance spread in metal-rich clusters is smaller than metal-poor ones (e.g. Pancino et al. 2017; Mészáros et al. 2020).

These open clusters are several orders of magnitude less massive than the typical old globular, and their metallicity is on average significantly higher (i.e. around solar instead of [Fe/H] $\lesssim -0.7$ dex). Both factors seem to attenuate the signal of the MPs found in Galactic globulars hindering any conclusions about the role age might play in the MP phenomenon. Fortunately, massive clusters have been forming in the Magellanic Clouds almost continuously for a Hubble time (cf. Glatt et al. 2009; Baumgardt et al. 2013). As these clusters are relatively metal poor, they provide the best opportunity to explore how the MPs express at different ages in a more controlled way.

Using a sample of Magellanic Clouds clusters Martocchia et al. (2018) showed that at a given cluster mass ($\sim 10^5$ $M_\odot$) the width of the RGB in colour–magnitude diagrams (CMDs) when using supercolours increases as a function of cluster age, suggesting the abundance variations present in the RGBs of older clusters are more severe than the ones found in the younger ones. Similar results are presented by Lagioia et al. (2019) in their fig. 10. These photometric findings are in agreement with spectroscopic studies like Hollyhead et al. (2019) showing N variations <1 dex at young ages (~ 2 Gyr) compared to the ones characteristic of old Galactic globulars which can comfortably exceed one dex (e.g. Cohen, Briley & Stetson 2005; Martell & Smith 2009; Pancino et al. 2010b).

However, Salaris et al. (2020) have shown that for RGB stars the comparison of the signals of N variations is not straight forward between clusters of different ages due to changes in the efficiency of the first dredge-up. Essentially, for a constant initial star-to-star N abundance difference, the observed N difference between subpopulations would appear to increase for increasing age. While this qualitatively matches observations, Salaris et al. found that the observed increase is stronger than the effect of the first dredge-up in their models, implying an intrinsic increase in N abundance with cluster age. However it is clear that evolutionary effects like this hamper any conclusions coming out of RGB stars regarding the role the cluster age plays in the initial star-to-star abundance variation.

To investigate the effect of this issue, in this paper we perform the critical step forward to study light-element abundance variations on the main sequence (MS), whose stars are not affected by evolutionary effects and preserve their initial chemical composition, and also avoiding the effects of stellar rotation. These abundance variations have been traced down to ~ 0.2 $M_\odot$ in old globulars, e.g. Milone et al. (2012). In this work we use deep imaging of NGC 419, a massive ($\sim 10^5$ $M_\odot$, Kamann et al. 2018), young (~ 1.4 Gyr, Glatt et al. 2009) Small Magellanic Cloud cluster with [Fe/H] $\sim$ -0.7 dex, in order to *search for MPs in stars in the same mass range where they are found in old globulars* (i.e. $\lesssim 1$ $M_\odot$ stars). The presence or absence of MPs in these stars will produce a clearer picture regarding the role cluster age plays in the manifestation of this phenomenon.

2 DATA AND MODELS

For NGC 419, we used *HST* images taken with the ACS/WFC and WFC3/UVIS cameras in bands *F336W*, *F343N*, *F438W*, *F555W*, and *F814W*[1] for our CMD analysis (programmes GO-10396, GO-12257, GO-14069, and GO-15061). We performed point spread function photometry and artificial star tests (ASTs) using DAOPHOT II and ALLFRAME (Stetson 1987, 1994) following the same procedure described in Bellazzini et al. (2002), Dalessandro et al. (2015), Martocchia et al. (2018) and references therein. For our study we focused on the stars within the half-light radius of NGC 419. We decontaminated the CMDs following the procedure outlined in Appendix A (cf. Fig. A1).

We use as reference clusters 47 Tuc (NGC 104), NGC 6352, and NGC 6637, all of them old Galactic globulars with a similar metallicity to NGC 419 (more on this in Section 3). The photometry for these clusters was taken from Nardiello et al. (2018, N18 from now on). The catalogues were cleaned by setting a $p > 95$ per cent cut in their membership probability based on their proper motions (cf. N18). Finally, we supplemented the N18 photometry of 47 Tuc with *Un* band and the deeper *B* from *HST* programme GO-15061. The *Un* band was not available for the other clusters in our sample.

We also make use the isochrones presented in Martocchia et al. (2017) on their analysis of NGC 419. These are 1.41 Gyr, [Fe/H] =-0.7 and include different chemical composition, namely, a scaled solar model ([C/Fe] = [N/Fe] = [O/Fe] =0.0); an intermediately N enhanced model ([C/Fe] = [O/Fe] =-0.1, [N/Fe] =$+0.5$); and an 'extremely' N enhanced model ([C/Fe] = [O/Fe] =-0.6, [N/Fe] =$+1.0$).

3 ANALYSIS

As mentioned above, our goal is to search for abundance variations characteristic of older clusters (i.e. MPs) using colours that are mostly sensitive to changes in N. Although stars in the MS have not experienced the first-dredge-up, we still need to proceed with care when selecting the sample of stars for this analysis to make sure that the signal of the N variations is not affected by different phenomena (at least in a significant way).

The CMD of NGC 419 reveals a great example of an extended MS turn-off (cf. Fig. 1). This feature is a prediction of stellar evolutionary models that include fast rotation rates (e.g. Brandt & Huang 2015; Niederhofer et al. 2015; Georgy et al. 2019; Gossage et al. 2019).[2] Rotationally induced mixing brings more hydrogen to the core of the stars (thus extending their MS lifetime), while the changes in the structure of the stars produce temperature gradients from the equator to the poles. The combination of both effects (prolonged MS time and a temperature dependence of the viewing angle of a star) introduce scatter in magnitude and colour in the turn-off of populations of stars with different rotation rates. The presence of large fractions of fast rotators in such clusters has been confirmed by a wide collection of studies (e.g. Bastian et al. 2017; Dupree et al. 2017; Kamann et al. 2018, targeting NGC 419; Milone et al. 2018).

---

[1]For simplicity we will refer to them as: *U*, *Un*, *B*, *V*, and *I*, respectively.
[2]Alternative (and less successful) interpretations of the extended MS turn-off phenomenon included: age spreads, abundance variations, and variable stars. Although each of these hypotheses had their merits, they all lacked the predictive power of the (confirmed) fast-stellar rotation hypothesis. See Cabrera-Ziri et al. (2018) for a brief review.
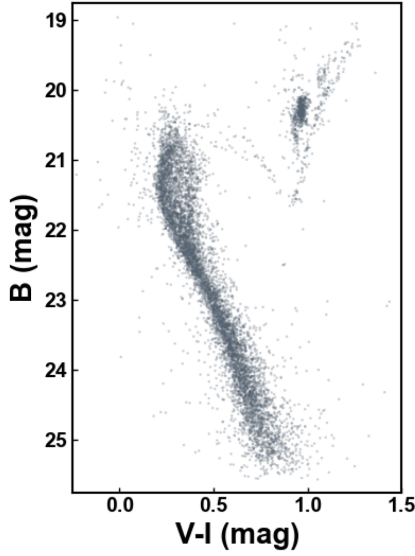
Figure 1. $V - I$ versus B CMD of NGC 419. The presence of fast rotating stars in this cluster can be inferred from the shape of the turn-off, see the text. The N surface abundance of these stars might not reflect the initial value (see the text). We will avoid these stars for our analysis.

Massive ($\gtrsim 1.3$ M$_\odot$ stars) MS stars that have been rotating fast will have altered surface abundances consequence of rotationally induced mixing (e.g. Hunter et al. 2008; Lagarde et al. 2012). This would affect elements like N (qualitatively) and cause N abundance variations similar to those seen in globular clusters – which do not seem to be explained by fast rotation (cf. Bastian & Lardo 2018; Cabrera-Ziri et al. 2018)

Hence we will focus our analysis on stars that should not have been affected by rotationally induced mixing (i.e. magnetically braked stars[3]) and that lie in parts of the CMD where stars of different chemical composition diverge significantly when using the right combination of filters. In Fig. 2 we can see that the isochrones with different composition start separating at magnitudes fainter than $B \sim 22$ mag. For our study, we will focus on the stars in the B-magnitude range from 23.5 to 25.5 mag, which correspond to the mass range between $1.05 \gtrsim$ M$_\odot \gtrsim 0.75$, according to our models.

We should note that we only use these models to inform us when populations with difference N variations start to become distinct. These models are not adequate for a direct comparison to the data in order to infer the presence/absence of MPs. For that we will use clusters with known MPs as empirical templates.

3.1 The signature of N variations in the MS

To start we have chosen 47 Tuc, a Galactic cluster with a similar metallicity to NGC 419 (i.e. [Fe/H] ~ -0.7 dex). In Fig. 3 we show different CMDs of 47 Tuc in the same bands of our NGC 419 photometry. We applied the distance modulus of NGC 419 to the absolute magnitudes of 47 Tuc in order to simplify the comparison between clusters, i.e. stars at a given apparent magnitude would share roughly similar masses (we adopted $m - M = 18.83$ mag from Rubele, Kerber & Girardi 2010 for NGC 419 and $m - M =$

---

[3]Stars with convective envelopes develop magnetic fields. These cause the wind to rotate as a solid body, transporting angular momentum outwards and slowing the rotation rate, cf. Kraft (1967).
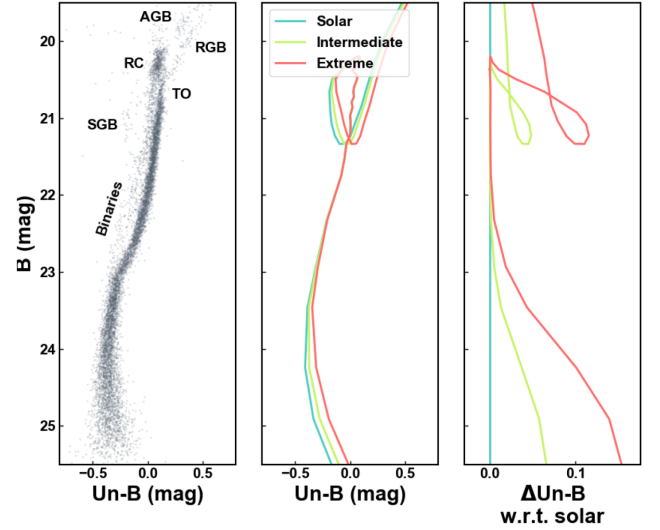

Figure 2. Left: A zoom into the MS of the $Un - B$ versus B CMD of NGC 419. For clarity we have identified some of the main evolutionary stages. Middle: Behaviour of models with different N enrichment in the $Un - B$ CMD. The blue, green, and red lines show the predictions of our isochrones with solar scaled, intermediate, and extreme N enhancement composition, respectively (cf. Section 2). Right: Colour difference between the solar scale and N enhanced isochrones as a function of magnitude. For $B > 22$ mag, the models start to diverge in the $U - B$ and $Un - B$ colours.
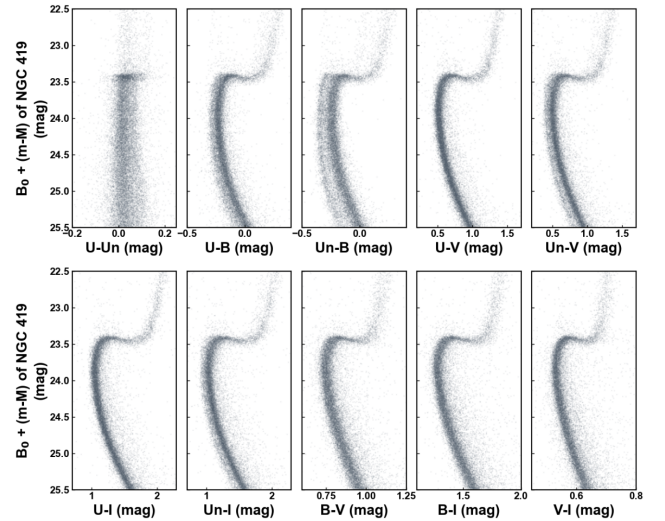

Figure 3. CMDs of 47 Tuc. We plot the CMDs at the same distance as NGC 419 so that stars of the same magnitude will have roughly similar masses. In $Un - B$, $Un - V$, and $Un - I$ colours, the difference between the solar scaled (blue MS) and N-rich population (red MS) is very clear.

13.266 mag from Gaia Collaboration 2018 for 47 Tuc). Note that colours containing the Un-band are very effective at separating the solar-scaled and N enhanced population. These two subpopulations are also appreciable in some colours containing the U-band (e.g. $U - B$), however, the distinction between the two is less clear.

The contrast between subpopulations with different chemical composition can be maximized in a colour–colour plot. For example, in the top panel of Fig. 4 we show the normalized colour–colour plot: $\Delta(Un - B)$ versus $\Delta(U - I)$ for 47 Tuc stars. These colours were normalized with respect to the mean of the colour distribution
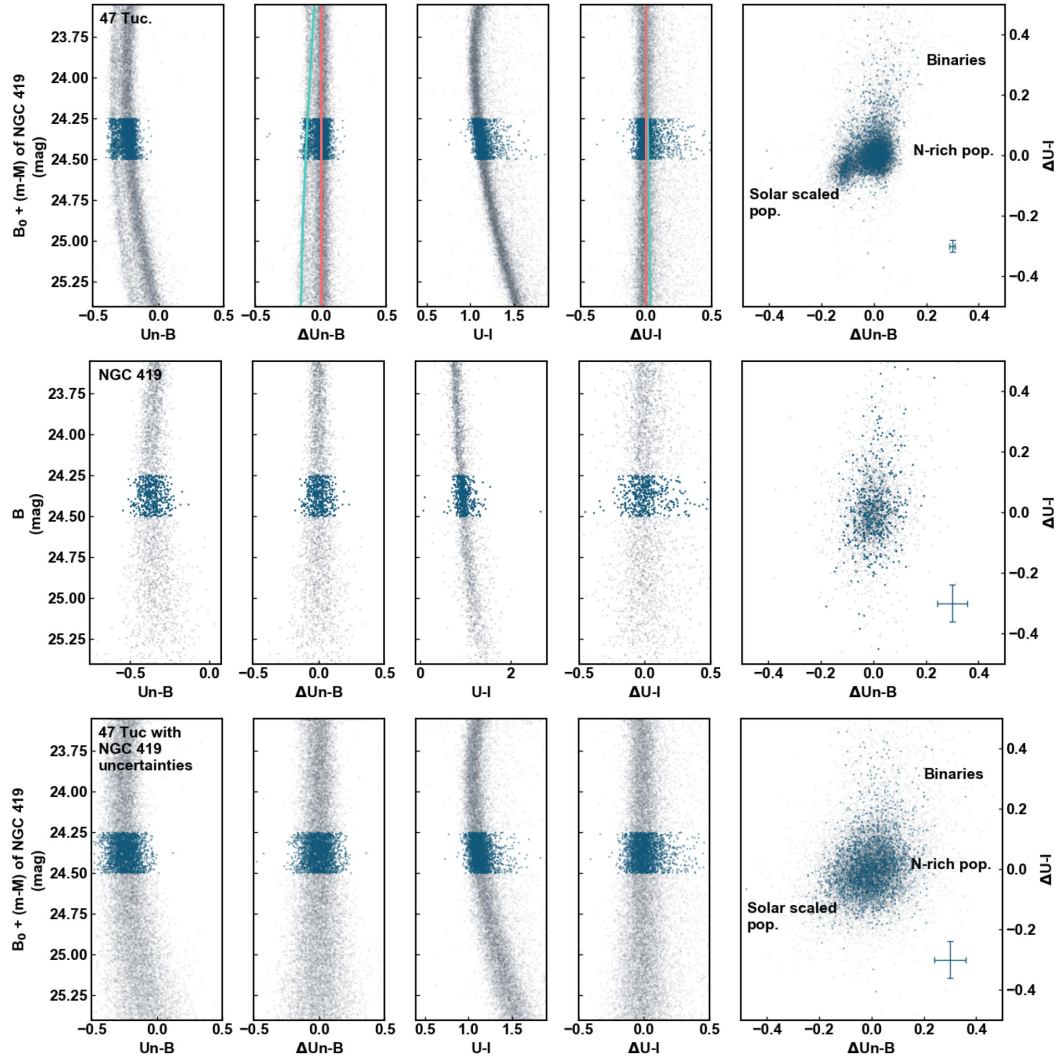
Figure 4. Top: Normalized CMDs and colour–colour plot of 47 Tuc. In this study we focus on stars in the entire range $23.5 < B < 25.5$ (grey points), however, to facilitate the comparison we highlighted in blue the stars in a narrow magnitude ($24.25 < B < 24.50$) range in the different panels. The solar scaled (blue) and 'extremely' N-rich (red) models are shown for reference in the first row. The solar scaled and N-rich population can be clearly identified in the $Un - B$ CMD, and in the $\Delta(Un - B)$ versus $\Delta(U - I)$ plot. In $U - I$ the binary stars are very prominent (red tail of the colour distribution); these can also be spotted in the normalized colour–colour plot. Middle: Similar to the top panel but for NGC 419. No clear evidence of multiple populations is found by visual inspection of the colour–colour plot. Bottom: Similar to the other panels but now showing a simulation of the CMD of 47 Tuc at the distance of NGC 419. In this case the photometric uncertainties blur the distinctions between the different subpopulations.

at every magnitude, allowing us to compare the relative behaviour of stars in parts of the CMDs with different slopes. The stars from each population occupy distinct loci in $\Delta(Un - B)$ versus $\Delta(U - I)$ (cf. top right panel of Fig. 4).

In the middle panels of Fig. 4 we show the equivalent plot for the NGC 419 data. No clear evidence of multiple populations is found by a visual inspection of this colour–colour plot. However, given its distance, the photometric uncertainties of NGC 419 are significantly larger than the ones of 47 Tuc, so it is not clear if one would have been able to pick multiple populations by visual inspection of its colour–colour plot. We can explore this by simulating how the CMD of 47 Tuc would look like if it had the same photometric uncertainties as NGC 419. For this, we added a random Gaussian scatter to our 47 Tuc catalogue in order to match the uncertainties inferred from our AST on the NGC 419 images. The resulting CMDs are shown in the bottom panel of Fig. 4. Although the stars in the colour–colour plot show a somewhat larger scatter than the

expected from the photometric uncertainties, the clear distinction between subpopulations has vanished and now the solar-scaled and N-rich populations are blended with each other.

By visual inspection the scatter in $\Delta(Un - B)$ from NGC 419 seems smaller than the one from 47 Tuc, see also the histogram in the top left panel of Fig. 5 and Table 1. So if the former were to host multiple populations, the N variations among its stars would be more subtle than the ones present in 47 Tuc (which show changes up to $\sim$1.5–1.7 dex e.g. Briley et al. 2004). One can argue that this would not be unexpected, as mentioned in Section 1 there is very strong evidence for a correlation between the cluster's present day mass and the degree of abundance variations, so in principle this would be entirely consistent with the fact that NGC 419 is about an order of magnitude less massive than 47 Tuc.

That said, we carried out a similar experiment this time comparing the normalized $\Delta(U - B)$ colour distribution of NGC 419 with that of two other Galactic globulars (known to host abundance
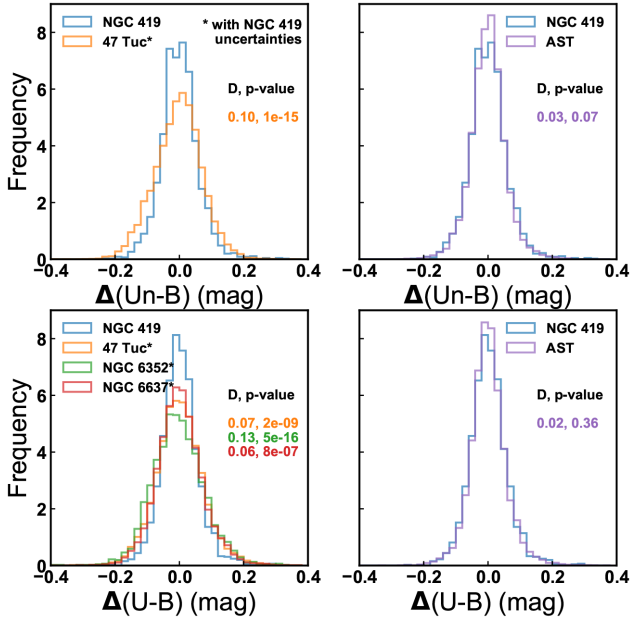
Figure 5. Comparison of the $\Delta(U-B)$ colour distributions of three clusters of similar metallicity as NGC 419. We are focusing on stars in the apparent B-magnitude range 23.5–25.5 (equivalent to $\sim$1–0.75 M$_\odot$). We report the KS-statistic, D, and p-value for the different cases (see the text). As in for the bottom panel of Fig. 4 random noise was added to the photometry of 47 Tuc, NGC 6352, and NGC 6637 to match the uncertainties of the NGC 419 data set, see the text.

Table 1. Standard deviation of colour distributions (in mag) of Fig. 5. We bootstrapped 10^4 times by resampling 500 stars in each iteration to derive the mean standard deviation of the colour distributions (values in table). The standard error estimated was ±0.003 mag for all distributions except for AST's $\Delta(Un-B)$ which was ±0.002 mag.

σ	AST	NGC 419	47 Tuc	NGC 6352	NGC 6637
$\Delta(Un-B)$	0.055	0.059	0.085	–	–
$\Delta(U-B)$	0.057	0.057	0.076	0.079	0.073

variations) with similar present day mass and metallicities: NGC 6352 and NGC 6637 ($\sim10^5$ M$_\odot$ and [Fe/H] ~-0.6; cf. Harris 1996; Baumgardt & Hilker 2018). As mentioned in Section 2, Un photometry was not available for these targets, however, from Fig. 3 we see that $U-B$ is also a good diagnostic for MPs.

Like for 47 Tuc before, we added random scatter to the catalogues of these clusters to match the uncertainties of NGC 419 data set. We then selected stars with $\sim$1–0.75 M$_\odot$ and in the bottom left panel of Fig. 5 we show their $\Delta(U-B)$ colour distribution.[4] The $\Delta(U-B)$ colour distributions of NGC 6352 and NGC 6637 are very similar to the one of 47 Tuc, and significantly wider than the distribution of NGC 419 (cf. Table 1).

That said, there is scaling relation between a globular cluster's mass and the severeness of their abundance variations (cf. Section 1). So, the narrow width of NGC 419's colour distributions with respect to 47 Tuc's could be accounted (at least in part) by

[4]We adopted $m-M=14.43$ and 15.28 for NGC 6352 and NGC 6637 respectively (Harris 1996). Since both clusters are severely affected by extinction, we corrected for differential reddening using the procedure described in Niederhofer et al. (2016).

this relation. Moreover, even though NGC 6352 and NGC 6637 currently have a similar mass to NGC 419, their initial mass might have been significantly larger in the past, which could explain their relatively wide colour distributions.[5]

For reference, in the right-hand panels of Fig. 5, we show a comparison between the $\Delta(U-B)$ and $\Delta(Un-B)$ colours expected from a single stellar population. For this we have used the catalogues generated in the AST. We used these catalogues to create the CMDs, which were normalized in the same way as the real data from the different clusters. The colour distributions from NGC 419 are clearly more consistent with what is expected from a single stellar population than from what is observed in clusters with known abundance variations of similar metallicity.

In each panel of Fig. 5 we also report the KS-statistic, D, and p-value for the different colour distributions.[6] We can reject the pairwise null hypothesis that the colour distributions of 47 Tuc, NGC 6352 and NGC 6637, and NGC 419 are drawn from the same parent population at the $p=10^{-3}$ level. However, we cannot say the same for the colour distributions of the AST catalogue (i.e. we cannot reject that they are 'drawn from the same distribution').

4 SUMMARY AND CONCLUSIONS

A growing number of studies have reported that the amplitude of the star-to-star abundance variations characteristic of globular clusters systematically changes as a function of global parameters like cluster's mass and metallicity. New spectroscopic and photometric evidence suggest the age of massive clusters also affects the way this phenomenon manifests, pointing towards more subtle signals at younger ages (cf. Section 1).

These studies were focused on RGB stars, however, where evolutionary effects like the first-dredge-up limit any conclusion regarding their *initial* N composition. This motivates the study of MS stars, i.e. stars which have not undergone these evolutionary effects. The best targets are the same type of low-mass stars ($\lesssim1$ M$_\odot$ – i.e. stars not affected by fast rotation as this could also affect their surface abundances) that populate the MS of old globulars.

For this work we have analysed different CMDs of low-mass stars ($\sim$0.75–1.05 M$_\odot$) of the young massive cluster NGC 419 ($\sim$1.4 Gyr, $\sim2\times10^5$ M$_\odot$) to look for evidence for primordial star-to-star N variations. All things being equal, in colours like $U-B$ and $Un-B$, the presence of such abundance variations would produce broader colour distributions than the ones expected for a cluster with homogeneous abundances.

We use the colour distribution of old clusters with known star-to-star N variations as empirical templates for our comparison with NGC 419. We find that the MS stars of NGC 419 display significantly narrower $U-B$ and $Un-B$ colour distributions than the same stars in our template clusters. Moreover, the colour

[5]Both NGC 6352 and NGC 6637 orbit closer to the Galactic centre than 47 Tuc and both NGC 6352 and NGC 6637 have shallow stellar mass functions (Baumgardt et al. 2019). Both of these argue towards NGC 6352 and NGC 6637 having lost more stellar mass than 47 Tuc.
[6]D is a measure of the maximum distance between the cumulative distributions of NGC 419 and the other clusters. While the p-value is the probability of obtaining test results at least as extreme as the results actually observed during the test, assuming that the null hypothesis is correct.

distributions of NGC 419 seem to be consistent with what is expected from a cluster with homogeneous abundances.[7]

These results have very interesting implications. Previous studies of integrated *J*-band spectra of very young (<30 Myr) massive ($\sim 10^6$ $M_\odot$) clusters have found no evidence for the type of abundance variations found in old globulars (cf. Cabrera-Ziri et al. 2016; Lardo et al. 2017). The integrated near-infrared spectra of such young clusters are dominated by the light of red supergiants (~ 8–35 $M_\odot$), these stars formed and followed a very different evolution than the low-mass ($\lesssim 1$ $M_\odot$) stars found in older globulars. So if the mechanisms responsible for the primordial abundance variations found in old globulars act only in low-mass stars, no evidence would be expected in red supergiants. A similar argument could be made for stars populating the RGB of young ($\lesssim 2$ Gyr) massive clusters, i.e. they are not the same kind of stars as the ones found to host MPs in old globulars (i.e. low-mass stars).

The results presented here suggest that even when comparing 'like-with-like' (i.e. the same kind of low-mass/long-lived stars), the abundance variations characteristic of old globulars (e.g. 47 Tuc, NGC 6352, and NGC 6637) appears to be significantly smaller or absent in this young cluster of similar metallicity (NGC 419). That said, we cannot conclude if this effect is driven mostly by its age or its mass. On one hand, there is a well-established correlation between the mass of a globular cluster and the strength of the signal of its abundance variations. This could explain in part why the colour distributions of NGC 419 are narrower than those of 47 Tuc ($\sim 10^6$ $M_\odot$). On the other hand, the study of young $\sim 10^6$ $M_\odot$ clusters has not produced evidence for MPs as mentioned above, suggesting the age of NGC 419 could also contribute to its apparent chemical homogeneity.

Finally we would like to emphasize that this work represents a case study on a single target. These results should be confirmed independently by different techniques and different targets. If confirmed (i.e. no/subtle-abundance variations), a possible explanation could be that MPs never occurred in recently formed clusters like NGC 419 because some special environmental conditions are not satisfied (e.g. low gas pressures/densities in the last couple of Gyr, cf. D'Ercole, D'Antona & Vesperini 2016; Elmegreen 2017), preventing the mechanisms required for the formation of MPs to operate.

Another alternative is that the process responsible to drive the formation of MPs still operates at young ages; however, it produces smaller fractions of N-enhanced stars and/or the N enhancements are very subtle. If evidence for (subtle) MPs is eventually found in this cluster, future hypothesis to explain the origin of MPs would need to explain why old clusters (~ 10 Gyr) of similar mass and metallicity show stronger signals of abundance variations, i.e. larger fraction of severely N-enhanced stars (e.g. 47 Tuc, NGC 6352, and NGC 6637).

ACKNOWLEDGEMENTS

REFERENCES

Bastian N., Lardo C., 2018, ARA&A, 56, 83
Bastian N. et al., 2017, MNRAS, 465, 4795
Baumgardt H., Hilker M., 2018, MNRAS, 478, 1520
Baumgardt H., Parmentier G., Anders P., Grebel E. K., 2013, MNRAS, 430, 676
Baumgardt H., Hilker M., Sollima A., Bellini A., 2019, MNRAS, 482, 5138
Bellazzini M., Fusi Pecci F., Montegriffo P., Messineo M., Monaco L., Rood R. T., 2002, AJ, 123, 2541
Brandt T. D., Huang C. X., 2015, ApJ, 807, 25
Briley M. M., Harbeck D., Smith G. H., Grebel E. K., 2004, AJ, 127, 1588
Cabrera-Ziri I., Lardo C., Davies B., Bastian N., Beccari G., Larsen S. S., Hernandez S., 2016, MNRAS, 460, 1869
Cabrera-Ziri I., Martocchia S., Hollyhead K., Bastian N., 2018, Mem. Soc. Astron. Ital., 89, 24
Carrera R., Martínez-Vázquez C. E., 2013, A&A, 560, A5
Carrera R., Pancino E., 2011, A&A, 535, A30
Carretta E., Bragaglia A., Gratton R. G., Recio-Blanco A., Lucatello S., D'Orazi V., Cassisi S., 2010, A&A, 516, A55
Cohen J. G., Briley M. M., Stetson P. B., 2005, AJ, 130, 1177
Dalessandro E., Ferraro F. R., Massari D., Lanzoni B., Miocchi P., Beccari G., 2015, ApJ, 810, 40
D'Ercole A., D'Antona F., Vesperini E., 2016, MNRAS, 461, 4088
de Silva G. M., Gibson B. K., Lattanzio J., Asplund M., 2009, A&A, 500, L25
Dupree A. K. et al., 2017, ApJ, 846, L1
Elmegreen B. G., 2017, ApJ, 836, 80
Gaia Collaboration, 2018, A&A, 616, A10
Georgy C. et al., 2019, A&A, 622, A66
Glatt K. et al., 2009, AJ, 138, 1403
Gossage S. et al., 2019, ApJ, 887, 199
Harris W. E., 1996, AJ, 112, 1487
Hollyhead K. et al., 2019, MNRAS, 484, 4718
Hunter I. et al., 2008, ApJ, 676, L29
Kamann S. et al., 2018, MNRAS, 480, 1689
Kraft R. P., 1967, ApJ, 150, 551
Kraft R. P., 1979, ARA&A, 17, 309
Lagarde N., Decressin T., Charbonnel C., Eggenberger P., Ekström S., Palacios A., 2012, A&A, 543, A108
Lagioia E. P., Milone A. P., Marino A. F., Cordoni G., Tailo M., 2019, AJ, 158, 202
Lardo C., Cabrera-Ziri I., Davies B., Bastian N., 2017, MNRAS, 468, 2482
Li C., Wang Y., Tang B., Milone A. P., Yang Y., Ji X., 2020, ApJ, 893, 17
MacLean B. T., De Silva G. M., Lattanzio J., 2015, MNRAS, 446, 3556
Martell S. L., Smith G. H., 2009, PASP, 121, 577
Martocchia S. et al., 2017, MNRAS, 468, 3150
Martocchia S. et al., 2018, MNRAS, 473, 2688
Mészáros S. et al., 2020, MNRAS, 492, 1641
Milone A. P. et al., 2012, ApJ, 754, L34
Milone A. P. et al., 2017, MNRAS, 464, 3636
Milone A. P. et al., 2018, MNRAS, 477, 2640
Monelli M. et al., 2013, MNRAS, 431, 2126
Nardiello D. et al., 2018, MNRAS, 481, 3382
Niederhofer F., Georgy C., Bastian N., Ekström S., 2015, MNRAS, 453, 2070

---

[7]We note that Li et al. (2020) came to similar conclusions with the same data set in a paper that appeared after the submission of this paper. In summary, they fitted synthetic clusters with different degrees of N abundance variations to the observations of low-mass MS stars of NGC 419. Likewise, they report that their simple stellar population model (i.e. homogeneous abundances) was the best at reproducing the observations. However they cannot exclude small ($\lesssim 0.2$ dex) variations in N abundance.

Niederhofer F., Bastian N., Kozhurina-Platais V., Hilker M., de Mink S. E., Cabrera-Ziri I., Li C., Ercolano B., 2016, A&A, 586, A148
Pancino E., Carrera R., Rossetti E., Gallart C., 2010a, A&A, 511, A56
Pancino E., Rejkuba M., Zoccali M., Carrera R., 2010b, A&A, 524, A44
Pancino E. et al., 2017, A&A, 601, A112
Rubele S., Kerber L., Girardi L., 2010, MNRAS, 403, 1156
Salaris M. et al., 2020, MNRAS, 492, 3459
Schiavon R. P., Caldwell N., Conroy C., Graves G. J., Strader J., MacArthur L. A., Courteau S., Harding P., 2013, ApJ, 776, L7
Smiljanic R., Gauderon R., North P., Barbuy B., Charbonnel C., Mowlavi N., 2009, A&A, 502, 267
Stetson P. B., 1987, PASP, 99, 191
Stetson P. B., 1994, PASP, 106, 250

APPENDIX A: FIELD STAR SUBTRACTION

We use a method similar to the one described in Niederhofer et al. (2016). Briefly, one defines a target region (in this case the cluster's centre) and a control field region (outskirts). The idea is that for every star in the control region, we flag a star in the cluster region that has a similar position in the CMD as a likely member of the field – accounting for the difference in solid angle (area) between the cluster and field regions.

The original method removes the closest star in the target region to the star in the control field. However, here we have implemented a variation where we create a probability distribution function (PDF) for the stars in the target region that is a function of their distance to the control field stars and their respective uncertainties. Then, the star to be flagged as likely member of the field is randomly chosen from this probability distribution.

To obtain the PDF we first need to calculate the distance d in colour magnitude space between a star from the target region and the star from the control region:

$$d = \sqrt{(\Delta\text{colour})^2 + (\Delta\text{magnitude})^2},$$

where Δcolour and Δmagnitude are the differences in colour and magnitude between the two stars. We also need the combined uncertainties in colour and magnitude given by

$$\sigma_c{}^2(\text{tot}) = \sigma_c{}^2(\text{target}) + \sigma_c{}^2(\text{control})$$

$$\sigma_m{}^2(\text{tot}) = \sigma_m{}^2(\text{target}) + \sigma_m{}^2(\text{control}),$$

here σ_c and σ_m are the respective standard deviations in the colour and magnitude for these stars. With this we calculate the total variance σ^2 and χ^2:

$$\sigma^{-2} = \frac{1}{\sigma_c{}^2(\text{tot})} + \frac{1}{\sigma_m{}^2(\text{tot})}$$

$$\chi^2 = d^2/\sigma^2,$$

then the PDF for each target star i would be

$$\text{PDF}_i = \frac{\mathcal{L}_i}{\sum_i \mathcal{L}_i},$$

where

$$\mathcal{L}_i = \frac{1}{\sqrt{2\pi\sigma_i^2}} \exp\left(-\frac{\chi_i^2}{2}\right).$$

In Fig. A1 we show the results of this procedure when applied to our NGC 419 data set. In pink we show the stars that have been flagged as likely members of the field and removed from the cluster CMD. The stars in the pink CMD are a representative sample of the stars in the control field CMD. The resulting decontaminated sample (right-hand panel) is the one used in our analysis in Section 3.

Furthermore, this method has the advantage that it enables us to calculate the probability of a given star to belong to the field. This is achieved by carrying out multiple realizations of this procedure and keeping track of the frequency each star is flagged as a likely field member. This is not possible in the Niederhofer et al. method as that method will always identify the same stars as field members if one repeats the procedure.

For example, in Fig. A2 we present different CMDs where the stars are colour coded by their probability to belong to the field. There probabilities were determined from 1000 realizations of our method and counting how many times a given star was flagged as a field member. In panel (a) we show the cluster region CMD before decontamination. Panels (b) and (c) present two alternative samples of field star contaminants, and below decontaminated CMDs using those samples – panels (a-b) and (a-c).

Panel (b) shows the same stars shown in pink in Fig. A1; these stars were flagged as field stars in one realization of our method. By removing these stars from the CMD shown in panel (a), we will obtain a relatively *pure* sample of cluster stars across all evolutionary phases. However, this method assumes that the stellar populations found in the control region are uniformly distributed across the entire field of view *and* that there are no cluster stars in the control region. Clearly this last assumption is not satisfied in our NGC 419
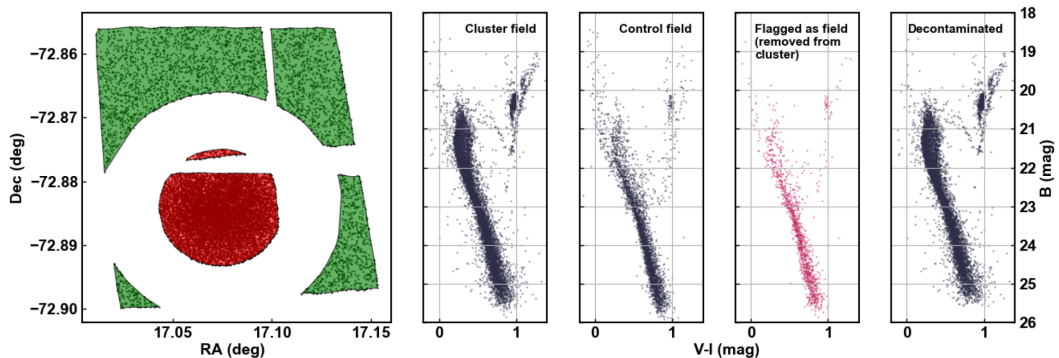

Figure A1. The left-hand panel shows the chosen regions in the sky for the cluster (red) and control field (green). Since the area ratio cluster to control fields is ∼0.37, for every star in the control field we flag ∼0.37 stars in cluster region as likely field members. The panels to the right show the CMDs of the centre, outskirts, stars chosen as contaminants (and removed from the cluster catalogue), and the decontaminated CMD. The stars from the latter are the ones used in our analysis (Section 3).
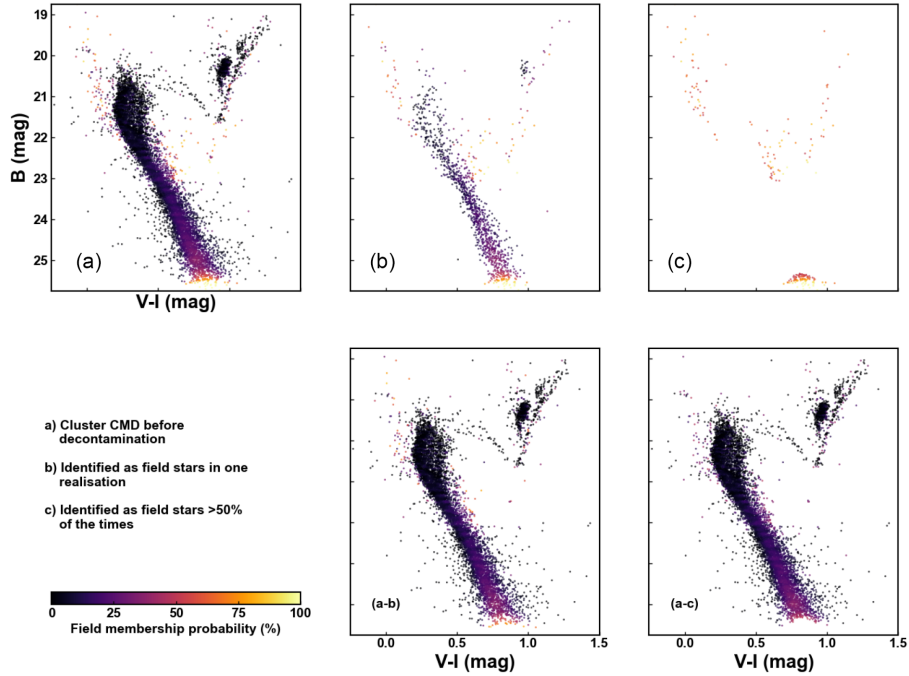
Figure A2. CMDs of the central region of NGC 419 with stars colour coded by their field membership probability derived from 1000 realizations of our decontamination technique. (a) CMD of cluster field. (b) Stars flagged as field in one realization of our method (i.e. pink CMD of Fig. A1). (c) Stars identified as field members > 50 per cent of our 1000 realizations. In the bottom row, we find the decontaminated CMDs by subtracting from (a) stars from (b) and (c). Panel (a-b) shows the same CMDs as the rightmost panels of Fig. A1, but for reference, now the stars are colour coded with their field membership probability. See the text for discussions.

data set (cf. control field CMD in Fig. A1), where we still have a non-negligible contribution of the cluster in our control region. This means that for a region like the cluster turn-off would tend to 'oversubtract' stars – the dark points in the turn-off region of (b) of Fig. A2 are likely cluster members.

On the other hand, if one were interested for example in a more *complete* sample of stars in the cluster turn-off (i.e. less oversubtraction), that could be achieved by simply setting a field membership probability threshold. In panel (c) of Fig. A2 we show an example of the stars with > 50 per cent chance of being field members. Removing those stars from the CMD we would minimize the oversubtraction of stars in the turn-off or RGB; however, this comes at the expense of the *purity* of the sample (it would have more contaminants).

We note that although this method folds in the uncertainties the photometry of both cluster and control field, if a certain part of the CMD is not well populated in your control/background sample, it will be very unlikely flagged as field member in your cluster CMD, e.g. outliers at the faint end (B > 23 mag) of the MS. As one would expect, the better the background sample one feeds in, the better result one gets out.

Having said that, given our limitations from the restricted *HST* pointings for this target a better alternative for the control field is not available. So any effort to decontaminate this data set from field stars will be compromised by this.

Finally, for our particular science case the choice of field decontamination method did not affect our conclusions, and the same results were found by subtracting stars by setting a 50 per cent cut in field membership probability (cf. Fig. A3), or by simply sampling of stars according to the field region CMD like in Fig. A1 and removing those from the cluster sample.
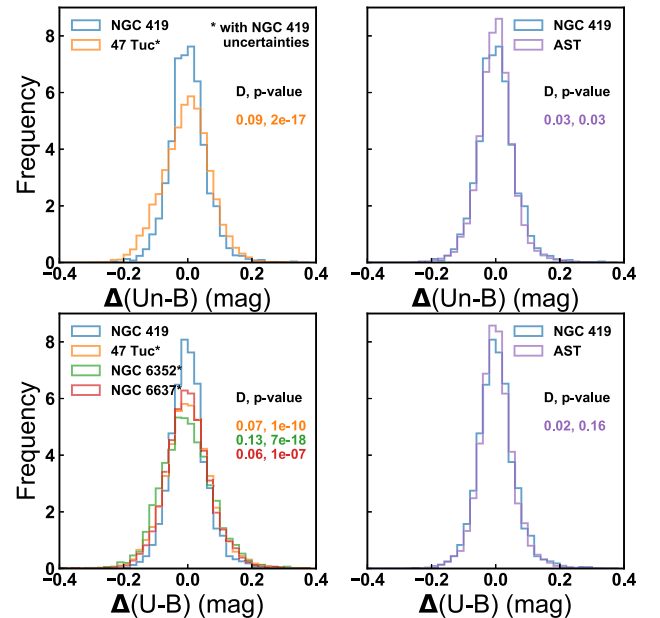
This paper has been typeset from a TEX/LATEX file prepared by the author.

Figure A3. Similar to Fig. 5. But instead of decontaminating our sample using the procedure outlined in Fig. A1 (i.e. one realization of our method), here we removed from the CMD of NGC 419 all stars with > 50 per cent probability to belong to the field – i.e. stars from panel (a-c) in Fig. A2. The results remain the same, i.e. the colour distributions of the other cluster are significantly wider than NGC 419.